

Bipolar Charge Storage Characteristics in Copper and Cobalt Co-doped Zinc Oxide (ZnO) Thin Film

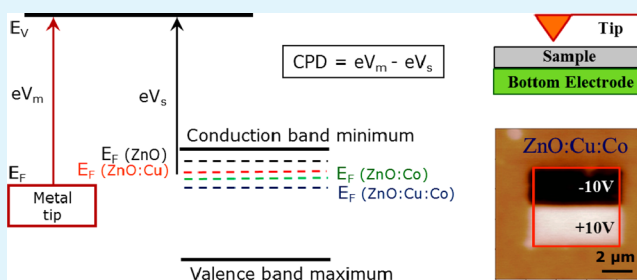
Amit Kumar,[†] Tun Seng Herng,[‡] Kaiyang Zeng,^{*,†} and Jun Ding[‡]

[†]Department of Mechanical Engineering, National University of Singapore, 9 Engineering Drive 1, Singapore 117576

[‡]Department of Materials Science and Engineering, National University of Singapore, 7 Engineering Drive 1, Singapore 117574

ABSTRACT: The bipolar charge phenomenon in Cu and Co co-doped zinc oxide (ZnO) film samples has been studied using scanning probe microscopy (SPM) techniques. Those ZnO samples are made using a pulsed laser deposition (PLD) technique. It is found that the addition of Cu and Co dopants suppresses the electron density in ZnO and causes a significant change in the work function (Fermi level) value of the ZnO film; this results in the ohmic nature of the contact between the electrode (probe tip) and codoped sample, whereas this contact exhibits a Schottky nature in the undoped and single-element-doped samples. These results are verified by Kelvin probe force microscopy (KPFM) and ultraviolet photoelectron spectroscopy (UPS) measurements. It is also found that the co-doping (Cu and Co) can stabilize the bipolar charge, whereas Cu doping only stabilizes the positive charge in ZnO thin films.

KEYWORDS: zinc oxide, codoped ZnO, Kelvin probe force microscopy, bipolar charge, charge stability



1. INTRODUCTION

Zinc oxide (ZnO) is an emerging semiconductor material for many applications in spintronics and microelectronics, because of its wide band gap.^{1–3} Various functional applications in ZnO have been achieved using the defect engineering and via the introduction of transition-metal ions.^{4–7} It is reported that copper (Cu)-doped ZnO has high resistivity because of electron trapping.⁸ A recent study on Cu-doped ZnO (ZnO:Cu) has shown that the solid solubility of Cu in ZnO was ~11 at.%.⁹ Furthermore, 8 at.% Cu-doped ZnO has shown multiferroic-like behavior⁹ and bipolar charging phenomena.¹⁰ It is reported that the 8 at.% Cu-doped ZnO thin film sample can store 20%–30% charge up to 20 h, but, unevenly, more than 50% of the charge decayed within the first 3 h of the discharging process.¹⁰

However, the limited solid solubility of Cu in ZnO has hampered the further development of ZnO:Cu samples for charge storage applications. To overcome this challenge, in this work, the ZnO:Cu (8 at.%) sample is further doped with cobalt (Co), since Co has high solid solubility into ZnO (~30 at.%).^{11–13} In order to determine the optimum amount of cobalt, several different concentrations of cobalt were first doped into ZnO:Cu (8 at.%), followed by X-ray diffraction (XRD) characterization to determine the crystallographic orientation of the samples. Figure 1 shows a comparison among the different samples based on their crystal structures. These results show that the higher concentrations of Co reduce the crystallinity in the samples. The peak corresponding to ZnO (002) becomes broader and weaker for the samples with more than 9 at.% Co concentration (as showed by the curve of 11 at.% Co). Therefore, the XRD results suggest that the 9 at.% Co

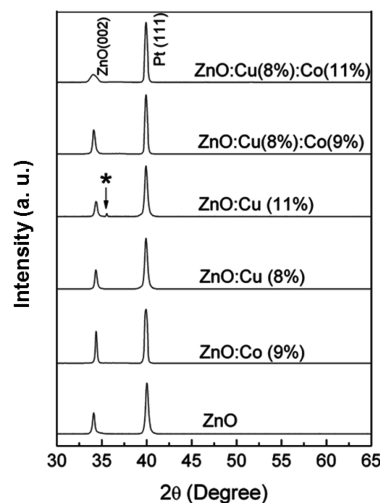


Figure 1. XRD intensity as a function of the angle 2θ for various concentrations of copper and cobalt in ZnO samples. The best crystallinity peak is found for the combination of 8% copper and 9% cobalt in the ZnO sample.

with 8 at.% Cu forms the better crystalline structure in ZnO, compared with that from other compositions. Therefore, based on these XRD results, in this work, four different composition samples are selected to study the charge stability in ZnO-based

Received: July 4, 2012

Accepted: September 4, 2012

Published: September 4, 2012



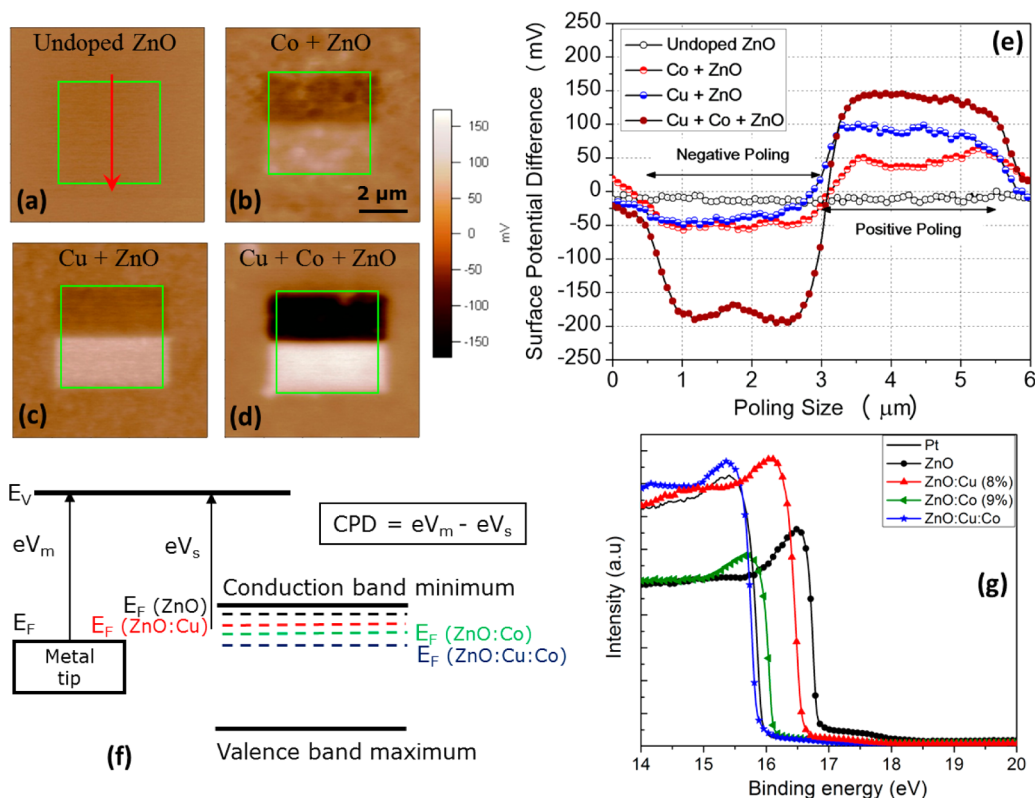


Figure 2. (a), (b), (c) and (d) Surface potential images immediate after application of the dc biases for the studied ZnO samples ((a) undoped ZnO, (b) ZnO doped with Co, (c) ZnO doped with Cu, and (d) ZnO doped with Cu and Co). The darker areas represent the decrease in the surface potential value and brighter (white) areas represent the increase in the surface potential value (on the same scales). (e) The surface potential changes (caused by dc biases) is plotted against poling size (measured at the arrow location) for all the samples. (f) Schematic diagram of flat band structure, also showing the location of the Fermi level for different samples. (g) UPS results data for Pt, ZnO, ZnO:Cu, ZnO:Co, and ZnO:Cu:Co samples.

thin films: i.e., undoped ZnO; ZnO:Co (9 at.%); ZnO:Cu (8 at.%); and ZnO:Cu (8 at.%):Co (9 at.%).

2. MATERIALS AND EXPERIMENTAL PROCEDURE

The pulsed laser deposition (PLD) technique was used to grow the four selected compositions (ZnO-based) thin films on (001) Si/SiO₂/Ti/Pt substrate; here, Pt is acting as a bottom electrode. All the samples were deposited at a temperature of 600 °C and an oxygen partial pressure of 2×10^{-4} Torr. The deposition targets were first prepared by mixing an appropriate amount of ZnO and CuO or CoO powder in a clean alumina mortar, followed by pressing and sintering at 1000 °C for 12 h to obtain the ZnO:Cu, ZnO:Co, and ZnO:Cu:Co targets with correct compositions. Two sets of samples with the selected compositions were deposited. After the deposition, the film samples were first characterized by energy-dispersive spectroscopy and X-ray photoemission spectroscopy to confirm the Cu or Co percentages. Furthermore, XRD characterizations were performed to determine the crystal structure of the films. The XRD results (Figure 1) show that the preferred texture is along the *c*-axis (002) for all of the samples and no secondary phase is detected within the limitation of XRD. The nominal thickness of the films is found to be ~ 240 nm. To study the charging characteristics, a commercial scanning probe microscopy (MFP-3D, Asylum Research, USA) is used for dc bias writing in contact mode and followed by contact potential measurement in Kelvin probe force microscopy (KPFM, noncontact) mode. A Pt-coated tip (tip radius ~ 15 nm) with a spring constant of ~ 2 N/m and a resonant frequency of ~ 70 kHz (Electric-Lever, Olympus, Japan) is used for all the measurements. Similar to the previous study,¹⁰ all the KPFM measurements are performed at 3 V ac voltage and a lift height of 40 nm. KPFM is a well-established technique that has been used to measure the contact potential between two surfaces brought in the vicinity.^{14–16}

To investigate the charge stability characteristics, positive and negative dc bias is applied to charge a small region of the sample surface by using a conducting tip. Thus, a charge pattern is created over an area of a few micrometers.¹⁷ Then KPFM is used to measure the contact potential change at different time intervals, using the same conducting tip.

To create a charge pattern, a positive (+10 V) and negative (−10 V or −5 V) dc biases are applied on a $5 \mu\text{m} \times 5 \mu\text{m}$ area using a 1 Hz line scan frequency by a conductive tip. Two different negative biases are used for transferring negative charge onto the sample surface because the resistivity levels among the samples are different. Undoped ZnO and ZnO:Co samples have lower resistivity value compare to that of the ZnO:Cu and ZnO:Cu:Co samples ($\sim 10^6$ and $\sim 10^7$ Ω cm, respectively). Therefore, a small negative bias (−5 V) is used for undoped ZnO and ZnO:Co samples to avoid any damage to sample surface, whereas a high negative bias (−10 V) is used for the ZnO:Cu and ZnO:Cu:Co samples. As the contact potential values are affected by the charges during tip–surface interaction and absorption layer in the ambient conditions,¹⁵ the contact potential value of the unbiased region is reset to 0 V for all the samples in order to compare the different results quantitatively. In this work, all of the KPFM measurements were made on three different locations on each sample and it is found that the results are consistent and independent of the measurement locations.

3. RESULTS AND DISCUSSION

The contact potential immediately after the dc bias for all the samples are shown in Figures 2a–d. Brighter or darker regions (relative to that of the unbiased region) in the contact potential images show an increase or decrease in the contact potential value due to the bias application. The co-doped sample shows the maximum change in the contact potential value, compared

Table 1. Measured Work Function by Ultraviolet Photoelectron Spectroscopy (UPS) and Contact Potential Difference (CPD) by Kelvin Probe Force Microscopy (KPFM)

sample description	Pt	ZnO	ZnO:Cu	ZnO:Co	ZnO:Cu:Co
work function (ϕ) by UPS (eV)	5.27	4.48	5.01	5.13	5.37
work function difference, $\phi_{\text{Pt}} - \phi_{\text{sample}}$ (meV)		790	260	140	-100
CPD by KPFM (meV)		560 ± 10	220 ± 7	118 ± 5	-115 ± 5
junction type		Schottky	Schottky	Schottky	ohmic

to that in the other samples, as observed by the image contrast (all images are taken on the same scale). Figure 2e shows a quantitative comparison of the contact potential values within the biased region (taken from the arrow location in Figure 2a). For the undoped ZnO sample, no significant change in the contact potential value is observed under the biased region, whereas for the ZnO:Co sample, a change of ~ 50 mV in the contact potential value is observed on both positive- and negative-biased regions. For ZnO:Cu sample, an uneven change in the contact potential value is observed: ~ 100 mV changes on the positive biased region are observed, whereas only ~ 50 mV on the negative biased region are observed. However, the ZnO:Cu:Co sample shows a very significant change in the contact potential value on the biased region (~ 150 mV under the positive bias and ~ 200 mV under the negative bias); this is almost 3-fold different from the contact potential changes, compared with that in the ZnO:Co sample.

In principle, the contact potential measured using the KPFM technique is the difference between the surface potential of metal tip (eV_m) and the film surface (eV_s) (see Figure 2f), which is defined as the contact potential difference (CPD). An application of bias on the sample surface results in the injection of holes (or electrons) into the sample surface, which shifts the Fermi energy level of the material. This results the increase (or decrease) of the contact potential value. The efficiency of injection (electrons or holes) depends on the work function difference between the tip and the sample surface; if the difference is smaller, the injection efficiency will be higher.¹⁰

Table 1 summarizes the contact potential values measured by KPFM before the application of dc bias. It is observed that undoped ZnO has the highest contact potential value (~ 560 mV), compared to that of the ZnO:Co (~ 118 mV) and ZnO:Cu (~ 220 mV) samples. However, the ZnO:Cu:Co sample shows the negative contact potential value (-115.45 mV). The high contact potential value for undoped ZnO sample shows a Schottky contact at the tip/sample interface. This Schottky contact forms a barrier on the interface and, therefore, charge transfer between the tip and the sample surface becomes difficult. Hence, less significant change in the contact potential value for undoped ZnO sample is observed. This is similar to the behavior of the undoped ZnO film reported previously.¹⁰ For the ZnO:Cu sample, since the contact potential value under unbiased conditions is less than that of the undoped ZnO sample, more electrons and holes can be injected into the sample surface, because of the reduced Schottky barrier height at the tip-sample junction.

For ZnO:Co sample, the unbiased contact potential is even less than that of the ZnO:Cu sample; therefore, the injection of electrons and holes on the sample surface should be even higher. Conversely, the contact potential value under positive bias for the ZnO:Co sample is less, compared to that of the ZnO:Cu sample. This is due to the high resistivity value of ZnO:Cu, compared to that of the ZnO:Co sample, which allows more charge to be stored as a polarization charge.

However, for both the ZnO:Cu and ZnO:Co samples, an uneven behavior in the contact potential value is observed when the sample was under the positive and negative bias, with positive bias causing more-significant changes. In the KPFM measurements, the contact potential measured on a biased surface includes the contribution of three major factors:¹⁰ (i) surface charge or screen charge, (ii) injection charge, and (iii) polarization charge. The polarization charge is due to the rotation of the electric dipoles under an applied electric field (if the material shows dielectric-type behavior). Therefore, the asymmetric changes in the contact potential for the ZnO:Cu sample is most likely due to the polarization and injection charge contributions. A similar asymmetric contact potential behavior was also observed when the sample surface is under positive and negative biases in the previous study.¹⁰ In this study, however, it is found that the positive bias causes more change in the contact potential value than that by negative bias, which is different from what has been previously reported.¹⁰ The reason for the different asymmetric behavior is most likely due to the two different methods used for applying the bias. In the previous work,¹⁰ a step writing method (the bias was changed from -8 V to 10 V, with an increment step of 2 V at every distance of $0.5 \mu\text{m}$) was used to apply bias on the sample surface; therefore, there may be some overlapping effects from prior-applied low-voltage bias. However, in this work, a single positive ($+10$ V) and a single negative (-10 V) bias is used on the lower and upper half of the square region for dc writing, and these may cause the different appearance in the contact potential changes by the application of the positive/negative bias.

For the ZnO:Cu:Co sample, as the unbiased contact potential becomes negative; the nature of the contact at the tip-sample interface, therefore, is ohmic contact. This is significantly different from what was observed in the other samples. This ohmic contact at the interface allows easy flow of the electrons and holes into the sample surface, because there is no barrier at the contact interface. In addition, the more-significant asymmetric behavior in contact potential under biased conditions is observed for this sample, similar to the case of ZnO:Cu sample under the biased condition. This is also due to the contributions of the injection and polarization charges to the contact potential (detailed discussion is included in the later portion of the paper). In order to further confirm the results of the KPFM measurements as well as the Schottky to Ohmic contact transition, ultrahigh-vacuum ultraviolet photoelectron spectroscopy (UPS) measurements are also performed on these samples to determine the energy band structure (Figure 2g). First, the work function of pure Pt substrate (reference sample) is measured by UPS, which is found to be ~ 5.27 eV. For undoped ZnO, the work function value is measured to be ~ 4.48 eV. Therefore, the work function difference from UPS measurement between the Pt and undoped ZnO is ~ 0.8 eV (see Table 1), which is in good agreement with the earlier reported value.² Second, the work function values measured by

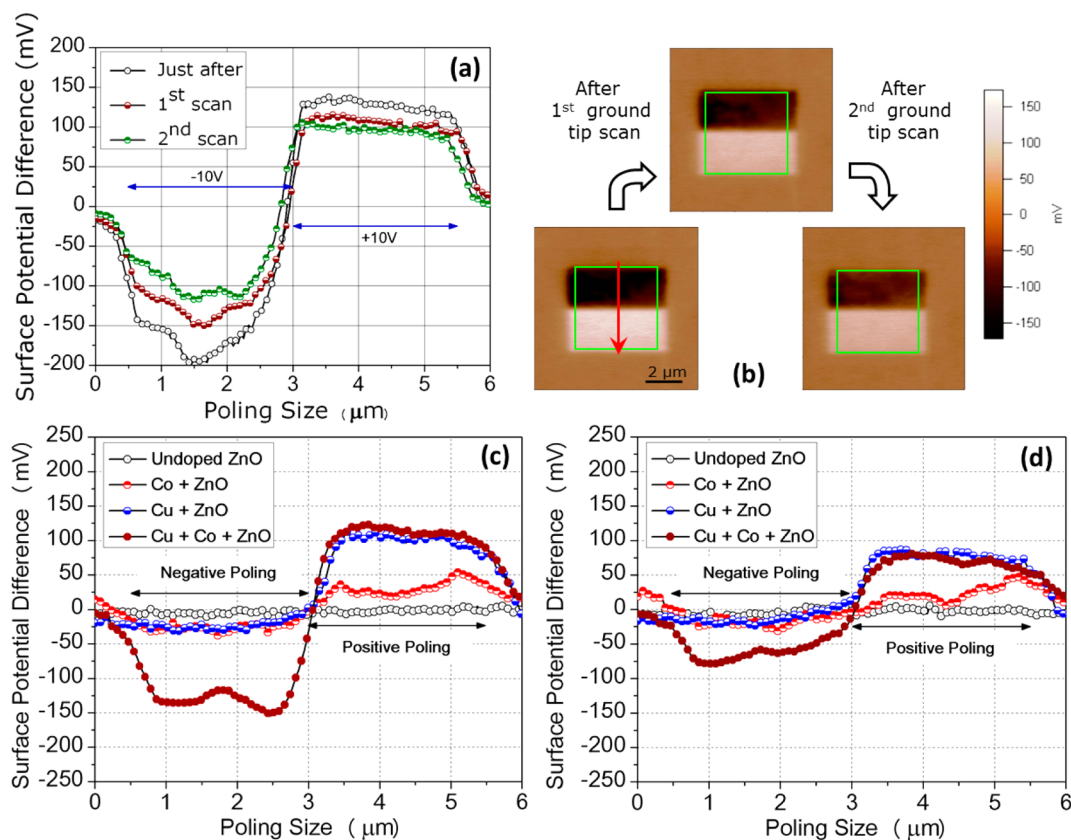


Figure 3. (a) Change in surface potential values for the ZnO:Cu:Co sample immediately after scanning, after the first grounded tip scan, and after the second grounded tip scan (measured at the red arrow location shown in panel b). (b) Surface potential image immediately after scanning, after the first grounded tip scan, and after the second grounded tip scan for the ZnO:Cu:Co sample. Also shown are the surface potential differences for all of the samples measured after (c) 2 h and (d) 20 h of bias application.

UPS for ZnO:Cu (~ 5.01 eV) and ZnO:Co (~ 5.13 eV) samples are found to be less than that of the Pt (~ 5.27 eV), which confirms a Schottky contact between the Pt-coated tip and the sample surface. Finally, the work function value for the ZnO:Cu:Co sample is found to be ~ 5.37 eV by UPS measurement and it is higher than that of the Pt; this results in an ohmic contact between the Pt-coated tip and the ZnO:Cu:Co sample. This observation is consistent with the KPFM measurement, which shows a negative unbiased contact potential (-115 meV) for the ZnO:Cu:Co sample (Table 1). These results show that a transition from Schottky to Ohmic contact is possible in the ZnO system via control of the Cu and Co co-doping.

Figure 2f schematically shows an energy band diagram for the ZnO-based samples that are in contact with the Pt-coated tip. The Fermi level of undoped ZnO is located at ~ 0.2 eV, close to the conduction band (CB) minimum.¹⁸ The electron density in the ZnO sample gets suppressed when Cu or Co is doped, because of electron trapping. The undoped ZnO has an electron concentration of $\sim 10^{19}$ cm^{-3} , which was further reduced by ~ 4 – 5 orders of magnitude with the incorporation of Cu or Co. This reduction in electron concentration shifts the Fermi level toward the valence band (VB) and, hence, reduces the work function difference between the Pt tip and sample surfaces (see Table 1). Interestingly, the Fermi level of the ZnO:Cu:Co sample has moved further toward the VB, which leads to the observed transition from Schottky to ohmic contact between the Pt tip and the sample.

To study the contributions of the polarization and injection charge to the contact potential, the ZnO:Cu:Co sample is again scanned with the grounded tip after the bias application. This grounded tip scan removes the contribution of surface charge in the contact potential measurement;¹⁰ therefore, the remaining contact potential is due to injection and polarization. Figures 3a and 3b show the contact potential variation and the images of the co-doped sample immediately after the bias application, as well as after the first and second grounded-tip scans. These results (Figures 3a and 3b) suggest that the measured contact potential includes the contribution of all three parts, i.e., injection, polarization, and surface charge. However, because a substantial quantity of charge is still presented on the sample surface, even after the second grounded tip scan, this suggests that the main contribution to the contact potential is the injected and polarization charge. In addition, it is observed that the more surface charge under the negatively biased region is removed by the grounded tip scanning, compared to that in the positively biased region. These observations indicate that, under the positive bias, the majority of charge is stored as injected and polarization charge.

To further study the charge stability in these ZnO-based samples, time-dependent charge decay tests are performed. For this test, the contact potential values of all the samples are measured at 2 and 20 h after the biases application (Figures 3c and 3d). For the undoped ZnO sample, the charge transferred to the sample surface disappears very fast, because the sample has high conductivity. For the ZnO:Co sample, more than 50% of the negative charge is decayed in the first 2 h and almost

completely disappeared after 20 h. This is because that the ZnO:Co sample is also very conductive and most of the charge is stored as surface charge in the negative bias region; therefore, it decays very fast. However, charge is still very stable in the positive bias region; even after 20 h, more than 50% of the charge is still stored in the sample. This shows the dominance of injected and polarized charge in the positively biased region, and these are very stable over time.

For the ZnO:Cu sample, the charge under negative bias is decayed in a similar way as that in the ZnO:Co sample, whereas the charge under positive bias becomes even more stable; 75% of the charge is still stored in the film after 20 h. On the other hand, for the ZnO:Cu:Co sample, as the initial amount of charge stored in the sample is higher, compared to those in the other samples; the initial charge decay rate is also noticeably higher within both of the positively and negatively biased regions, respectively. This is most likely due to the presence of a larger quantity of surface charge, which is transferred due to the Ohmic contact in the positively and negatively biased regions. In addition, it is observed that the decay rate is reduced significantly after the surface charge decay in the first 2 h. After 20 h, a similar amount of charge is stored in the positive bias region for the ZnO:Cu:Co sample as those in the ZnO:Cu sample. However, in the negative bias region, a substantial amount of charge is still stored in the ZnO:Cu:Co sample, which is significantly different from the charge storage behavior exhibited by the samples with only Cu or Co doping. This result suggests that the Cu and Co co-doped ZnO sample is more suitable for bipolar charge storage applications.

4. SUMMARY AND CONCLUSIONS

In summary, this work shows that the bipolar charge can be stored in the Cu and Co co-doped ZnO thin film. Cu doping stabilizes the positive charge in ZnO for a long time and Co doping can improve the negative charge stability. The contact potential measurement proves that the nature of contact between the SPM Pt-coated tip and the co-doped ZnO sample is changed to an ohmic nature from the Schottky contact. Therefore, a large quantity of charge (both positive and negative charges) can be stored in the sample. In addition, the ZnO:Cu:Co sample has higher resistivity, which gives rise to the polarization in the material. When an external bias is applied on the sample surface, a greater amount of charge can be stored as polarization and injection charge rather than the surface charge, which provides the stability to positive as well as negative charge in the co-doped ZnO sample for a longer time.

AUTHOR INFORMATION

Corresponding Author

*Tel.: +65-6516-6627. Fax: +65-6779-1459. E-mail: mpezk@nus.edu.sg.

Notes

The authors declare no competing financial interest.

ACKNOWLEDGMENTS

The authors would like to thank the support of National University of Singapore for this work. In particular, A.K. and K.Y.Z. acknowledge the support by MoE AcRF R-265-000-305-112. J.D. and TSH acknowledge the support by NRF-CRP R284-000-056-281.

REFERENCES

- (1) Liu, C.; Yun, F.; Morkoc, H. *J. Mater. Sci.: Mater. Electron.* **2005**, *16*, 555.
- (2) Özgür, U.; Alivov, Y. I.; Liu, C.; Teke, A.; Reshchikov, M. A.; Doğan, S.; Avrutin, V.; Cho, S. J.; Morkoc, H. *J. Appl. Phys.* **2005**, *98*, 041301.
- (3) Yang, Y. C.; Song, C.; Zeng, F.; Pan, F.; Xie, Y. N.; Liu, T. *Appl. Phys. Lett.* **2007**, *90*, 242903.
- (4) Liu, C.; Yun, F.; Morkoc, H. *J. Appl. Phys.* **2005**, *16*, 555.
- (5) Joseph, M.; Tabata, H.; Kawai, T. *Appl. Phys. Lett.* **1999**, *74*, 2534.
- (6) Yang, Y. C.; Zhong, C. F.; Wang, X. H.; He, B.; Wei, S. Q.; Zeng, F.; Pan, F. *J. Appl. Phys.* **2008**, *104*, 064102.
- (7) Lin, Y. H.; Ying, M.; Li, M.; Wang, X.; Nan, C. W. *Appl. Phys. Lett.* **2007**, *90*, 222110.
- (8) Furukawa, A.; Ogasawara, N.; Yokozawa, R.; Tokunaga, T. *Jpn. J. Appl. Phys.* **2008**, *47*, 8799.
- (9) Herg, T. S.; Wong, M. F.; Qi, D. C.; Yi, J. B.; Kumar, A.; Huang, A.; Kartawidjaja, F. C.; Smadici, S.; Abbamonte, P.; Sánchez-Hanke, C.; Shannigrahi, S.; Xue, J. M.; Wang, J.; Feng, Y. P.; Rusydi, A.; Zeng, K. Y.; Ding, J. *Adv. Mater.* **2011**, *23* (14), 1635.
- (10) Wong, M. F.; Herg, T. S.; Zhang, Z. K.; Zeng, K. Y.; Ding, J. *Appl. Phys. Lett.* **2010**, *97*, 232103.
- (11) Ueda, K.; Tabata, H.; Kawai, T. *Appl. Phys. Lett.* **2001**, *79*, 988.
- (12) Park, J. H.; Kim, M. G.; Jang, H. M.; Ryu, S. W.; Kim, Y. M. *Appl. Phys. Lett.* **2004**, *84*, 1338.
- (13) Hsu, H. S.; Huang, J. C. A.; Huang, Y. H.; Liao, Y. F.; Lin, M. Z.; Lee, C. H.; Lee, J. F.; Chen, S. F.; Lai, L. Y.; Liu, C. P. *Appl. Phys. Lett.* **2006**, *88*, 242507.
- (14) Kalinin, S. V.; Bonnell, D. A. *Phys. Rev. B* **2001**, *63*, 125411.
- (15) Kim, Y.; Bae, C.; Ryu, K.; Ko, H.; Kim, Y. K.; Hong, S.; Shin, H. *Appl. Phys. Lett.* **2009**, *94*, 032907.
- (16) Zhang, Q.; Kim, C. H.; Jang, Y. H.; Hwang, H. J.; Cho, J. H. *Appl. Phys. Lett.* **2010**, *96*, 152901.
- (17) Terris, B. D.; Stern, J. E.; Rugar, D.; Mamin, H. J. *Phys. Rev. Lett.* **1989**, *63*, 2669.
- (18) Janotti, A.; Walle, C. C. V. *Rep. Prog. Phys.* **2009**, *72*, 126501.